The anti-biofouling properties of thin-film composite nanofiltration membranes grafted with biogenic silver nanoparticles

Shasha Liu[a], Fang Fang[a], Jun Jie Wu[b], Kaisong Zhang[a]*

[a] *Key Laboratory of Urban Pollutant Conversion, Institute of Urban Environment, Chinese Academy of Sciences, Xiamen 361021, China*

[b] *School of Engineering and Computing Sciences, Durham University, Durham DH1 3LE, UK*

* Corresponding author: K. S. Zhang, Tel/ Fax: +86 592 6190782. Email: kszhang@iue.ac.cn

ABSTRACT: Biofouling is still one of the most challenging issues of nanofiltration. One of the practical strategies to reduce biofouling is to develop novel anti-biofouling membranes. Herein, biogenic silver nanoparticles ($BioAg^0$-6) with the averaged diameter of only 6nm were firstly grafted on the surface of polyamide NF membrane. The effect of grafted $BioAg^0$-6 on the performance of thin-film composite (TFC) NF membranes was systematically investigated with a comparison to the grafted chemical AgNPs. $BioAg^0$-6 grafted membrane (TFC-S-BioAg) increased the hydrophilicity of the TFC membrane and water permeability, while maintaining the relatively high salt rejection. The result of silver leaching experiment indicated that the grafted $BioAg^0$-6 had a better stability on the membranes, the ratio of remained silver in the TFC-S-BioAg membrane was 95%, after soaked in pure water for 50 days. After 4 months immersion, the rejection of TFC-S-BioAg membrane remained more than 90% of initial rejection. The results of disk diffusion test revealed that both of TFC-S-BioAg membrane and TFC-S-ChemAg membrane showed effective anti-bacterial ability to inhibit P.aeruginosa and E.coli growth, the TFC-S-BioAg membrane showed more excellent and longer lasting antibacterial property. Therefore, $BioAg^0$-6 grafed TFC membranes could be potential as an effective strategy to decrease biofouling in nanofiltration process.

KEYWORDS: *biogenic silver nanoparticles; chemical silver nanoparticles; biofouling; antibacterial; nanofiltration*

1. INTRODUCTION

Biofouling is one of the most challenging problems in membrane separation processes which hinders wider applications of thin-film composite (TFC) nanofiltration (NF) membrane in wastewater treatment system[1, 2]. Biofouling begins with the bacterial adhesion on the membrane surface[3]. Once bacterial attaches to the membrane surface, bacteria will produce a bio-film, which is difficult to be eliminated and often cause irreversible damage to membrane structure with the decline in the permeate quantity[4, 5]. Antifouling strategies of TFC membranes are normally carried out either by feed stream pretreatment, cleaning-in-place program or by membrane surface modification[6, 7]. Physical pretreatment and chemical pretreatment are able to control inorganic and part of the organic fouling. However, most antifouling efforts by pretreatments are not effective in eliminating biofouling in membrane separation process[8]. The application of biocide such as chlorine in the feed stream was reported, which could effectively decrease the membrane biofouling. However, even 99.99% removal of bacteria from the feed water cannot guarantee the elimination of bacteria growth on the membrane surface because the remaining bacterial can still migrate and multiply rapidly[9]. Besides, the biocides added in the feed streams have often been found to damage the membrane structure[10]. Hence, the most immediate method to control biofouling is applying antifouling efforts to membranes directly.

Inorganic additives were incorporated into polymeric membranes with the purpose

of reducing membrane fouling[11-13]. Silver compounds and silver ions have been known to exhibit strong inhibitory and bactericidal effects as well as a broad spectrum of anti-microbial activities[14]. Due to their excellent biocidal properties and low toxicity towards mammalian cells[15, 16], silver nanoparticles (AgNPs) have been widely applied in TFC reverse osmosis (RO) membrane fabrication. Lee et al. [17] added AgNPs in the oil phase to form polyamine thin-film layer during the interfacial polymerization. Kim et al.[18] combined AgNPs into the aqueous solution during the interfacial polymerization to improve antifouling properties of TFC membrane. AgNPs were also attached to the surface of TFC membrane effectively via covalent banding, and the AgNPs showed good stability[19]. These reports indicated that AgNPs could be immobilized to the TFC membrane effectively and improved the antibacterial and antifouling properties. AgNPs with diameter of 15~100 nm are reported to synthesize via chemical reduction method, which is the most commonly used[20]. However, chemically produced silver nanoparticles often have problems with particles stability and tend to aggregate at high concentrations or when the average particle size is less than 40 nm[21].

In our previous work, novel biogenic silver nanoparticles were obtained using dried *Lactobacillus fermentum* biomass[22, 23]. The biogenic AgNPs with an average diameter of ~6 nm (Bio-Ag^0-6) exhibited excellent antibacterial performance. Some studies suggested that the antibacterial properties of AgNPs might be size dependent, with smaller particles having a greater bactericidal effect[24]. But the smaller AgNPs

synthesized in traditional approaches are often less stable than larger ones and tend to aggregate faster at high concentrations[25]. For Bio-Ag^0-6, the attachment of bacterium fragment on the surface of nanoparticles might prevent the AgNPs from aggregating. Therefore, Bio-Ag^0-6 showed a very high stability in aqueous solution[22], which is the advantage that normal chemical particles cannot afford.

In this study, Bio-Ag^0-6 was grafted onto the surface of freshly fabricated TFC NF membrane for the first time, in contrast with the commercial chemical AgNPs. The AgNPs showed good stability on the surface of TFC membrane though chemical covalent bonds. The surface of freshly prepared membranes were investigated by scanning electron microscopy (SEM), energy dispersive X-ray spectroscopy (EDS), attenuated total reflectance Fourier transform infrared (ATR-FTIR) spectroscopy and water contact angle apparatus. The silver release from the membranes in both static immersion and dead-end filtration were evaluated. Furthermore, the AgNPs grafted membranes were soaked in pure water for 4 months to assess the effect of silver release on the long term filtration performance. The antibacterial and antibiofouling performances were also evaluated by the disk diffusion method and bacterial suspension filtration experiment.

2. EXPERIMENTAL SECTION

Materials. Polysulfone (PS Solvay P3500) was bought from BASF (China) Co. Ltd. polyvinylpyrrolidone (PVP-K30), N-Methyl pyrrolidone (NMP; ≥99%)

triethylamine (TEA; ≥99%), sodium dodecyl sulfate (SDS; 99%), N-hexane (99%), sodium sulfate (Na_2SO_4; 99%), Ammonia solution (analytical grade), silver standard solution (1000 mg L^{-1}) were supplied by Sinopharm Chemical Reagent Co., Ltd.. Silver nitrate ($AgNO_3$; analytical grade) was purchased from Shanghai Shenbo Chemical Co., Ltd. Bovine serum albumin (BSA, 67 KDa), cysteamine (H_2N-$(CH_2)_2$-SH, 95%), Piperrazine (PIP; 99%), and trimesoyl chloride (TMC; 98%) were purchased from Aladdin Co. Ltd. Chemical AgNPs (diameter of 20 nm, 99.95%) were purchased from Beijing Dk Nano technology Co. Ltd.

Preparation of PS supporting membrane. The PS support membrane was prepared via immersion precipitation phase inversion method. Firstly, the blend solution was prepared by dissolving 17.5 wt.% PS, 0.5 wt.% PVP-K30 in NMP at 80 °C. After stirring for 12 h, the homogeneous solution was kept at the room temperature to remove air bubbles for around 12 h. Then the dope solution was casted onto a non-woven fabric (thickness 120 μm) using a casting knife, followed by dipping the membrane into a DI water bath for immediate phase inversion. The wet film thickness was controlled at ~220 μm. After 30 min in a gelation medium, the membrane was taken out and kept in DI water.

Synthesis and characterization of biogenic silver nanopaticles (Bio-Ag^0-6). The biogenic silver nanopaticles (Bio-Ag^0-6) was synthesized with *Lactobacillus fermentum* LMG 8900 as reported in a previous work[22, 26]. The detailed procedure was as followed: dried biomass was dissolved to in Milli-Q water in an Erlenmeyer flask,

with NaOH and diamine silver added sequentially. The final concentration of biomass, silver and $[OH]^{-1}$ were controlled to 10 g L^{-1}, 10 g L^{-1} and 0.2 mol L^{-1} respectively. After incubating in a shaking incubator at 30 °C (200 rpm) for 24 h, the solution was centrifuged at 5,000 rpm for 6 min. The biogenic silver hydrosol was separated and centrifuged at 6,000 rpm for 10 min for further concentration and purification. Finally, the biogenic AgNPs with diameter of 6 nm was obtained.

Preparation of TFC NF membranes. The TFC NF membrane was prepared by interfacial polymerization of PIP and TMC as described elsewhere[27]. Firstly, the PS support layer was immersed in a 1.6 wt% PIP aqueous phase for 1 min. The excess solution was removed from the soaked surface by a rubber roller. Then the organic solution of TMC (0.35 wt.%) in n-hexane was poured over the membrane for 20 s to finish the interfacial polymerization reaction. The PS membrane was taken out from the n-hexane solution and heated in an oven at 50□ about 3 min, for a better polymerization reaction. Finally, the prepared TFC membranes were rinsed with pure water and then ethanol before the surface grafting.

Newly fabricated TFC membranes were immediately immersed in a H_2N-$(CH_2)_2$-SH ethanol solution (20 mM, 40 mL) for 6 h. Then the membranes (labeled as TFC-S) were moved out from the ethanol solution, washed with pure ethanol and DI water, and incubated with the selective layer in contact with biogenic AgNPs, chemical AgNPs suspension (0.1 mM, 40 mL) for 12 h, respectively. Finally, the membrane samples (labeled as TFC-S-BioAg, TFC-S-ChemAg) were rinsed with

DI water and store in DI water for future tests.

Membrane characterization. Surface morphologies of the composite membranes were observed by a field emission scanning electron micro-scope (FESEM, HITACHI S-4800) equipped with an X-ray energy dispersive spectroscope (EDS) system. The accelerating voltage of SEM is 5 kV. Before SEM analysis, all membrane samples were dried in vacuum oven at 80□ for more than 48 h and then coated with gold. Presence of silver nanoparticles was confirmed by energy dispersive X-ray spectra (EDS) and elemental mapping.

Functional groups of membrane surfaces were identified by ATR FT-IR spectroscopy, which was conducted on the Nicolet iS10 (Thermo Fisher Scientific) equipped with multi-reflection Smart Performer ATR accessory. All spectra included the wave numbers from 500 to 4000 cm^{-1} with 64 scans at a resolution of 4.0 cm^{-1}.

Hydrophilicity of the membrane surface was assessed according to the pure water contact angle, which was measured by the sessile drop method on a video contact angle system (DSA100, German KRUSS). The contact angle was measured automatically by a video camera in the instrument using the drop shape analysis software. At least five measurements on different locations of each sample were performed to calculate an averaged value of contact angles.

The filtration performances of the composite membranes were evaluated by a dead-end filtration cell (Model 8010, Millipore Corp. USA). The membranes (4.1cm^2 of effective area) were operated at 0.35 MPa. Pure water flux was measured by the

weight of permeate water at a constant transmembrane pressure. The weight of the permeate flux was recorded by a precision electronic balance (Denver Instrument, USA). 2000 ppm Na_2SO_4 was used as feeding solutions to test membranes rejection. Pure water flux and salt rejection were calculated with Eqs.(1) and (2), respectively.

$$F = \frac{W_p}{At} \quad (1)$$

$$R = \left(1 - \frac{C_p}{C_f}\right) \times 100\% \quad (2)$$

Where F is the permeate flux (L/m^2h), W_p the permeate volume (L), A the membrane area (m^2), t the filtration time (h), R the rejection ratio, and Cp and Cf the conductivities of permeate and feed solution, respectively. All the results presented are average data with standard deviation from at least three samples of each type of membrane.

Stability of the immobilized silver. The stability of the immobilized silver on the prepared composite nanofiltration membrane was evaluated via both static release and filtration experiments. In the static release test, the composite nanofiltration membrane was cut into a circular shape with an area of 3.5 cm^2, and was subsequently soaked in a sealed flask filled with 10 ml of Milli-Q water at room temperature. As specified time intervals, the water samples were collected and acidified by 2% HNO_3 to be analyzed by inductively coupled plasma mass spectrometry (ICP-MS, Agilent, model 7500CX).

The silver release rate under the filtration condition was evaluated by driving DI water through the membrane at a constant pressure of 0.35 MPa. The permeate water

was collected every 1.0 h and released silver concentration by ICP-MS as described above.

Further, the effect of silver depletion on the change of composite membranes filtration performance was also studied. First, the initial pure water flux and Na_2SO_4 rejection of the composite membranes were measured. Then the membranes were immersed in DI water for 4 months to maximize the release of silver. After that, the pure water flux and Na_2SO_4 rejection were tested again. Based on the data before and after immersion, the flux and the rejection variation can be calculated.

Antibacterial assessment. In the disk experiment, *Pseudomonas aeruginosa (ATCC27853)* and *Escherichia coli (ATCC15597)* was inoculated into a liquid lysogeny broth (LB) and incubated in an Incubator Shaker (Zhicheng, ZHWY-2012C) shaking at 180 rpm for 10 h at 37□. The resulting cell suspensions were further diluted to approximately 10^6 colony-forming units (CFU)/mL. Aliquots (100 μL) of the diluted working suspension inoculated with *P. aeruginosa* and *E.coli* were applied to agar plates, respectively. Membrane samples (diameter 2.1 cm) were then placed onto the nutrient agar plates with the selective layer in contact with the agar surface. After incubation at 37□ for 24 h, the bacterial inhibition zone of each plate was observed. There are at least three parallel samples for each type of membrane.

During SEM investigation, membrane samples with size of 2 cm^2 were immersed in 25 mL of *P. aeruginosa* and *E.coli* suspensions (3.0×10^5 CFU/mL) for 8 h at 37□. Then the membrane samples were dried in an oven at 80□ for 24h, and coated with

platinum using sputter coater for SEM observation.

3. RESULTS AND DISCUSSION

Characterization of membranes. The surface morphologies of original, thiol modified, biogenic silver immobilized and chemical silver immobilized membranes are shown in Fig. 1. All of these membranes exhibited typical "ridge and valley" structure characteristic of the PA thin-film layer[19]. There were no obvious differences between them. However, the high resolution SEM images showed spherical particles located on the TFC-S-BioAg and TFC-S-BioAg membrane surface evenly. The particles located on the TFC-S-BioAg membrane ranged from 5~10 nm in diameter, about the size with that of biogenic AgNPs. There were several spherical particles on the surface of TFC-S-ChemAg membrane sample, the diameters of these particle were about 20 nm, about the size with that of chemical AgNPs. Furthermore, the EDS spectra results indicated that the biogenic and chemical AgNPs were successfully grafted on the selective layer of the TFC membranes. As shown in Fig. 2, carbon, oxygen and sulfur picks are available in the all samples, but picks associated with the silver nanoparticles are available only in TFC-S-BioAg and TFC-S-ChemAg membranes (Fig. 2b and c).

The chemical structure of the selective layer was analyzed by FT-IR spectroscopy, a convenient method to analyze the various chemical bonds in the outermost part of a membrane. The spectra of the PS support membrane and various TFC membranes are

presented in Fig. 3. Beside the typical PS bonds of the substrate, the spectrum of the composite membranes exhibited the absorption peaks at 1620 cm^{-1} and weak broad adsorption bands at 3420 cm^{-1} ,which were attributed to the stretching vibration band of the amide C=O groups and N-H stretching vibration, respectively[28]. Meanwhile, the peaks at 1441 cm^{-1} was associated to C=O stretching and O-H bending of carboxylic acid. These characteristic bands proved that the polyamide was formed on the surface of PS substrate during the interfacial polymerization reaction. However, the characteristic peak of S-H stretching located near 2540-2560 cm^{-1} did not show up. This may because of the low sensitivity of thiol group in FT-IR due to the high polarizability of sulfur[29].

The contact angle is a measure of tendency for water to wet the membrane surface. As can be seen from Fig. 4, the static water contact angle decreased from 77 ± 5.9° (that of PS membrane) to 42.5 ± 2.2° (that of bare TFC membrane). The main chemical components in the selective layer affecting the hydrophilicity of the membrane are amide groups, amino end groups and carboxylic acid groups (from the hydrolysis of unreacted acyl chloride groups). After grafting H_2N-$(CH_2)_2$-SH, the contact angle slightly decreased to 39.4 ± 3.0°, suggesting the attachment of thiol groups on membrane surface slightly improve the surface hydrophilicity. The contact angles of membrane with grafted biogenic and chemical AgNPs decreased to 37.0± 4.5° and 37.5±2.6° . The decrease in contact angle by the grafted AgNPs is generally accord with the results in other literature[5, 18]. Lower contact angle means

stronger hydrophilicity. It has been demonstrated that more hydrophilic surface can decrease bacterial adhesion and protein adsorption[30, 31]. The increased hydrophilicity of the membranes could decrease the water contact angles and increase the water flux[32], which would be discussed in next section.

The main chemical components in the selective layer affecting the hydrophilicity of the membrane are amide groups, amino end groups (from the hydrolysis of unreacted acyl chloride groups), and AgNPs. The improved surface hydrophilicity of the TFC membrane prepared from a polymerization reaction of PIP and TMC is mainly from the AgNPs content at the surface skin layer.

Water filtration performance of membranes. The pure water flux and the salt rejection of membranes are presented in Fig. 5. The grafted cysteamine and AgNPs on the composite membranes effectively enhanced the pure water flux. At a constant pressure of 0.35MPa, the pure water flux of the bare TFC, TFC-S, TFC-S-BioAg, and TFC-S-ChemAg membranes were 13.24±1.44 L/m^{2}h, 17.41±1.52 L/m^{2}h, 17.39±3.02 L/m^{2}h, 17.41±0.69 L/m^{2}h, respectively, and Na_2SO_4 rejection was 86.89±2.10%, 85.47±2.47%, 87.03±0.99%, 86.15±5.48 %, respectively. The higher water flux and slight influence of salt rejection for the grafted membranes could be due to the the increased hydrophilicity and the effects of ethanol solution used in the grafting procedure. A mild solvent such as ethanol could increase the water flux of TFC membranes without salt rejection[33]. Ethanol solution could lead to membrane swelling and wipe out small molecular fragments, so a more loose structure can be formed but

still not enough to markedly decrease salt rejection.

Effect of silver leaching. The stable and strong bond between the AgNPs and the membrane is important for ensuring the maintenance of anti-biofouling performance for high-efficient and eco-friendly membrane system[34]. The release rate of silver from the AgNPs grafted membrane was examined in both static and filtration experiments. The result of static immersion test was presented in Fig. 6, the initial rate of silver ions released from TFC-S-BioAg and TFC-S-ChemAg membrane were 0.024 and 0.17 μg cm^{-2} day^{-1}, respectively, and then declined steadily with time. After soaking in Milli-Q water for 50 days, the release rate of biogenic AgNPs and chemical AgNPs both leveled off to a level below 0.02 μg cm^{-2} day^{-1}. The total amounts of AgNPs grafted on the surface of TFC-S-BioAg and TFC-S-ChemAg membrane were 0.38 and 2.28 μg cm^{-2}, respectively. After 50 days of the static release test, the ratio of the remained silver to the original one on the TFC-S-BioAg and TFC-S-ChemAg membrane were 95% and 74%, respectively. According to the relatively low leaching rate less than 0.02μg cm^{-2} day^{-1}, the TFC-S-BioAg membrane is expected to last more than 340 days before all silver on the membranes completely released. This will potentially extend the anti-fouling effect of the TFC membrane. It can be concluded that the TFC-S-BioAg membrane has a more stable and durable anti-biofouling performance than TFC-S-ChemAg membrane.

The concentration of silver ions in the permeate fluid during filtration experiment was analyzed by ICP-MS. The result is presented in Fig. 7. The leaching Ag^{+}

concentration in the permeate side was very low with the initial Ag^+ concentration being less than 29 ppb for the TFC-S-BioAg membrane, and less than 32 ppb for the TFC-S-ChemAg membrane. Then the release rate of Ag^+ gradually decreased as more water was filtered with time. According to the National Secondary Drinking Water Regulations, the Ag threshold is limited to 100 ppb. Hence, the amount of silver released from both the TFC-S-BioAg and the TFC-S-ChemAg membrane, has no health concern. According to the filtration experiment, both of the TFC-S-BioAg and the TFC-S-ChemAg membrane could be good choices for membrane biofouling disinfection since the Ag^+ release was below the threshold value during the filtration process.

Although the anti-bacterial action by silver nanoparticles is not fully studied, several researchers inferred that the anti-bacterial capacity of the composite membranes based on the ability to release biotoxic silver ions (Ag^+) to the surrounding solution [35]. Several studies have proved that the anti-bacterial capacity of silver loaded membranes had a significant reduction due to the decrease of the silver content [36]. In this study, most of the silver remained in the AgNPs grafted membranes, even 50 days after the soaking experiment.

To investigate the influence of silver leaching to the membrane filtration property, pure water flux and Na_2SO_4 rejection of membranes before and after treatment by 4 months immersion were measured. As shown in Fig. 8, the water flux (F_1) of all the membrane samples witnessed almost 40% increase compared to the initial flux (F_0).

With the increase of water flux, the Na_2SO_4 rejection (R_1) of the pristine TFC membrane decreased to 89% of the initial rejection (R_0), While the rejection of the TFC-S-BioAg and TFC-S-ChemAg membranes were 89.23% and 91.24%, respectively. The result indicated that the silver depletion from the surface of TFC-S-BioAg and TFC-S-ChemAg membranes does not influence the filtration performance obviously. The result that the salt rejection of AgNPs contained TFC membranes were higher than the bare TFC membranes, which is possible due to the antibacterial ability of the AgNPs.

Anti-biofouling performances of the Bio-Ag^0-6/PES composite membranes. *P. aeruginosa* and *E.coli* were selected as the tested bacterial strains model to assess the anti-biofouling activity of TFC membranes by the inhibition zone method. As depicted in Fig. 9, there was no clear antibacterial zone around the pristine TFC membrane, indicating no anti-biofouling activity against either *P. aeruginosa* or *E.coli*. However, after being grafting of the silver nanoparticles on membrane surfaces, both the TFC-S-BioAg and TFC-S-ChemAg membranes showed clear inhibition zones surrounding the samples. This illustrated that the antibiofouling activity of AgNPs grafted TFC membrane was derived from the silver nanoparticles[3]. The inhibition zone of TFC-S-BioAg menbrane is wider and clearer than that of TFC-S-ChemAg membrane, indicating that the antibacterial ability of the TFC-S-BioAg membrane is superior to the TFC-S-ChemAg membrane.

Chemically produced AgNPs often have problems in particle stability and tend to

aggregate at high concentrations or when the average particle size is less than 40 nm. However, the Bio-Ag^0-6 showed high stability in aqueous solution in this study. The attachment of the nanoparticles with the micro scale surface of the bacterium on which they were formed prevents them from aggregating. So the membrane embedded with Bio-Ag^0-6 may have a better anti-fouling property than the membrane embedded with chemical AgNPs.

The anti biofouling performance of the prepared membranes were investigated with a high concentration of stationary phase bacteria suspensions (~10^8 CFU/mL) in 8 h immersion test. The membrane samples were submerged in aqueous suspensions of *P. aeruginosa* and *E.coli.*, respectively. SEM images (Fig. 10) were obtained after removing membrane samples from the bacterial suspensions. As showed in Fig. 10(a), the *P. aeruginosa* bacterial with approximately 2 μm in length attached on the bare TFC membrane surface. On the contrary, TFC-S-BioAg and TFC-S-ChemAg membrane surfaces were relatively cleaner. The similar antifouling result for *E.coli.* was obtained in Fig. 10(b). This result suggested that both of the TFC-S-BioAg and TFC-S-ChemAg membranes presented excellent anti-bacterial and biofouling properties.

The mechanism of anti-biofouling activity of silver nanoparticles had still not been well understood. Some researches explained that the anti-bacterial capacity of silver composite membranes mainly relies on their ability to release silver ions (Ag^+), which has a strong toxicity to bacteria. Silver ions can react with cysteine by replacing the

hydrogen atom of the thiol group to form S-Ag complexes[37], thus hindering the respiratory function of the affected protease and preventing the DNA replication. Furthermore, Ag^+ can influence the structure and the permeability of the cell membrane [38, 39].

4. CONCLUSIONS

Biogenic AgNPs and chemical AgNPs were successful grafted onto the surface of polyamide TFC nanofiltration membrane with cysteamine as the bridging agent. Both of the TFC-S-BioAg and TFC-S-ChemAg membrane showed enhanced hydrophilicity and water flux, while maintaining good salt rejection. The TFC-S-BioAg membrane showed both better stability of embedded AgNPs and better antibacterial ability compared with the TFC-S-ChemAg membrane. Furthermore, 4 months immersion experiment demonstrated that AgNPs depletion did not influence the separation property of TFC membrane. The results demonstrated that biogenic AgNPs (Bio-Ag^0-6) could be used as an effective biocide agent to mitigate TFC membrane biofouling.

AKNOWLEDGEMENTS

KSZ thanks Royal Academy of Engineering, UK for the Research Exchange with China/India scheme. The authors gratefully acknowledge the financial support of

Xiamen Municipal Bureau of Science and Technology (3502Z20131159).

REFERENCES

(1) Minhas, F. T.; Memon, S.; Bhanger, M. I.; Iqbal, N.; Mujahid, M. Solvent Resistant Thin Film Composite Nanofiltration Membrane: Characterization and Permeation Study. *Appl. Surf. Sci.* **2013**, *282*, 887-897.

(2) Ben-Sasson, M.; Lu, X.; Bar-Zeev, E.; Zodrow, K. R.; Nejati, S.; Qi, G.; Giannelis, E. P.; Elimelech, M. In Situ Formation of Silver Nanoparticles on Thin-film Composite Reverse Osmosis Membranes for Biofouling Mitigation. *Water Res*. **2014**, *62*, 260-270.

(3) Li, J. H.; Shao, X. S.; Zhou, Q.; Li, M. Z.; Zhang, Q. Q. The Double Effects of Silver Nanoparticles on the PVDF Membrane: Surface Hydrophilicity and Antifouling Performance. *Appl. Surf. Sci.* **2013**, *265*, 663-670.

(4) Li, J. H.; Yan, B. F.; Shao, X. S.; Wang, S. S.; Tian, H. Y.; Zhang, Q. Q. Influence of Ag/TiO2 Nanoparticle on the Surface Hydrophilicity and Visible-light Response Activity of Polyvinylidene Fluoride Membrane. *Appl. Surf. Sci*. **2015**, *324* , 82-89.

(5) Koseoglu-Imer, D. Y.; Kose, B.; Altinbas, M.; Koyuncu, I. The Production of Polysulfone (PS) Membrane with Silver Nanoparticles (AgNP): Physical Properties, Filtration Performances, and Biofouling Resistances of Membranes. *J.Membr.Sci.* **2013**, *428*, 620-628.

(6) Yang, H. L.; Lin, J. C.; Huang, C. Application of Nanosilver Surface Modification to RO Membrane and Spacer for Mitigating Biofouling in Seawater Desalination. *Water Res*. **2009**, *43* , 3777-86.

(7) Chuo, T. W.; Wei, T. C.; Chang, Y.; Liu, Y. L. Electrically Driven Biofouling Release of a Poly(tetrafluoroethylene) Membrane Modified with an Electrically Induced Reversibly Cross-linked Polymer. *ACS Appl. Mater. Interfaces* **2013**, *5*, 9918-25.

(8) Pontié, M.; Rapenne, S.; Thekkedath, A.; Duchesne, J.; Jacquemet, V.; Leparc, J.; Suty, H. Tools for Membrane Autopsies and Antifouling Strategies in Seawater Feeds: A Review. *Desalination* **2005**, *181*, 75-90.

(9) Liu, C. X.; Zhang, D. R.; He, Y.; Zhao, X. S.; Bai, R. Modification of Membrane Surface for Anti-biofouling Performance: Effect of Anti-adhesion and Anti-bacteria Approaches. *J. Membr. Sci.* **2010**, *346*, 121-130.

(10) Kim, D.; Jung, S.; Sohn, J.; Kim, H.; Lee, S. Biocide Application for Controlling Biofouling of SWRO Membranes-An Overview. *Desalination* **2009**, *238*, 43-52.

(11) Huang, J.; Arthanareeswaran, G.; Zhang, K. Effect of Silver Loaded Sodium Zirconium Phosphate (nanoAgZ) Nanoparticles Incorporation on PES Membrane Performance. *Desalination* **2012**, *285*, 100-107.

(12) Jin, L.; Shi, W.; Yu, S.; Yi, X.; Sun, N.; Ma, C.; Liu, Y. Preparation and Characterization of a Novel PA-SiO2 Nanofiltration Membrane for Raw Water Treatment. *Desalination* **2012**, *298*, 34-41.

(13) Lee, H. S.; Im, S. J.; Kim, J. H.; Kim, H. J.; Kim, J. P.; Min, B. R. Polyamide Thin-film Nanofiltration Membranes Containing TiO2 Nanoparticles. *Desalination* **2008**, *219*, 48-56.

(14) Song, J.; Kang, H.; Lee, C.; Hwang, S. H.; Jang, J. Aqueous Synthesis of Silver Nanoparticle Embedded Cationic Polymer Nanofibers and Their Antibacterial Activity. *ACS Appl. Mater.*

Interfaces **2011**, *4*, 460-465.

(15) Choi, O.; Deng, K. K.; Kim, N.-J.; Ross Jr, L.; Surampalli, R. Y.; Hu, Z. The Inhibitory Effects of Silver Nanoparticles, Silver Ions, and Silver Chloride Colloids on Microbial Growth. *Water Res.* **2008**, *42*, 3066-3074.

(16) Danilczuk, M.; Lund, A.; Sadlo, J.; Yamada, H.; Michalik, J. Conduction Electron Spin Resonance of Small Silver Particles. *Spectrochim. Acta, Part A* **2006**, *63*, 189-191.

(17) Lee, S. Y.; Kim, H. J.; Patel, R.; Im, S. J.; Kim, J. H.; Min, B. R. Silver Nanoparticles Immobilized on Thin Film Composite Polyamide Membrane: Characterization, Nanofiltration, Antifouling Properties. *Polym. Adv. Technol.* **2007**, *18*, 562-568.

(18) Kim, E. S.; Hwang, G.; Gamal El-Din, M.; Liu, Y. Development of Nanosilver and Multi-walled Carbon Nanotubes Thin-film Nanocomposite Membrane for Enhanced Water Treatment. *J. Membr. Sci.* **2012**, *394*, 37-48.

(19) Yin, J.; Yang, Y.; Hu, Z.; Deng, B. Attachment of Silver Nanoparticles (AgNPs) onto Thin-film Composite (TFC) Membranes through Covalent Bonding to Reduce Membrane Biofouling. *J. Membr. Sci.* **2013**, *441*, 73-82.

(20) Jiang, H.; Moon, K. S.; Zhang, Z.; Pothukuchi, S.; Wong, C. Variable Frequency Microwave Synthesis of Silver Nanoparticles. *J. Nanopart. Res.* **2006**, *8*, 117-124.

(21) Mafuné, F.; Kohno, J. Y.; Takeda, Y.; Kondow, T.; Sawabe, H. Structure and Stability of Silver Nanoparticles in Aqueous Solution Produced by Laser Ablation. *J. Phys. Chem. B* **2000**, *104*, 8333-8337.

(22) Zhang, M.; Zhang, K.; De Gusseme, B.; Verstraete, W.; Field, R. The Antibacterial and

Anti-biofouling Performance of Biogenic Silver Nanoparticles by Lactobacillus Fermentum. *Biofouling* **2014**, *30*, 347-357.

(23) Zhang, M.; Field, R.; Zhang, K. Biogenic Silver Nanocomposite Polyethersulfone UF Membranes with Antifouling Properties. *J. Membr. Sci.* **2014**. *471*, 274-284.

(24) Morones, J. R.; Elechiguerra, J. L.; Camacho, A.; Holt, K.; Kouri, J. B.; Ramirez, J. T.; Yacaman, M. J., The Bactericidal Effect of Silver Nanoparticles. *Nanotechnology* **2005**, *16*, 2346-2353.

(25) Kim, Y. H.; Lee, D. K.; Cha, H. G.; Kim, C. W.; Kang, Y. S. Synthesis and Characterization of Antibacterial Ag-SiO2 Nanocomposite. *J. Phys. Chem. C* **2007**, *111*, 3629-3635.

(26) Zhang, M.; Zhang, K.; De Gusseme, B.; Verstraete, W. Biogenic Silver Nanoparticles (Bio-Ag0) Decrease Biofouling of Bio-Ag0/PES Nanocomposite Membranes. *Water Res*. **2012**, *46*, 2077-2087.

(27) Xiang, J.; Xie, Z.; Hoang, M.; Ng, D.; Zhang, K. Effect of Ammonium Salts on the Properties of Poly(piperazineamide) Thin Film Composite Nanofiltration Membrane. *J. Membr. Sci.* **2014**, *465*, 34-40.

(28) Li, Y.; Su, Y.; Dong, Y.; Zhao, X.; Jiang, Z.; Zhang, R.; Zhao, J., Separation Performance of Thin-film Composite Nanofiltration Membrane through Interfacial Polymerization Using Different Amine Monomers. *Desalination* **2014**, *333*, 59-65.

(29) Wharton, C. W. Infra-red and Raman Spectroscopic Studies of Enzyme Structure and Function. *Biochem. J.* **1986**, *233*, 25-36.

(30) Mazumder, S.; Falkinham III, J. O.; Dietrich, A. M.; Puri, I. K. Role of Hydrophobicity in

Bacterial Adherence to Carbon Nanostructures and Biofilm Formation. *Biofouling* **2010**, *26*, 333-339.

(31) Zhao, W.; Huang, J.; Fang, B.; Nie, S.; Yi, N.; Su, B.; Li, H.; Zhao, C. Modification of Polyethersulfone Membrane by Blending Semi-interpenetrating Network Polymeric Nanoparticles. *J. Membr. Sci.* **2011**, *369*, 258-266.

(32) Yang, Q.; Xu, Z. K.; Dai, Z.-W.; Wang, J. L.; Ulbricht, M. Surface Modification of Polypropylene Microporous Membranes with a Novel Glycopolymer. *Chem. Mater.* **2005**, *17*, 3050-3058.

(33) Kulkarni, A.; Mukherjee, D.; Gill, W. N. Flux Enhancement by Hydrophilization of Thin Film Composite Reverse Osmosis Membranes. *J. Membr. Sci.* **1996**, *114*, 39-50.

(34) Park, S. Y.; Chung, J. W.; Chae, Y. K.; Kwak, S. Y. Amphiphilic Thiol Functional Linker Mediated Sustainable Anti-Biofouling Ultrafiltration Nanocomposite Comprising a Silver Nanoparticles and Poly(vinylidene fluoride) Membrane. *ACS Appl. Mater. Interfaces* **2013**, *5*, 10705-10714.

(35) Cao, X.; Tang, M.; Liu, F.; Nie, Y.; Zhao, C. Immobilization of Silver Nanoparticles onto Sulfonated Polyethersulfone Membranes as Antibacterial Materials. *Colloids.Surf.,B* **2010**, *81*, 555-562.

(36) Chou, W. L.; Yu, D. G.; Yang, M. C. The Preparation and Characterization of Silver-Loading Cellulose Acetate Hollow Fiber Membrane for Water Treatment. *Polym. Adv. Technol.* **2005**, *16*, 600-607.

(37) Basri, H.; Ismail, A.; Aziz, M. Polyethersulfone (PES)-Silver Composite UF Membrane:

Effect of Silver Loading and PVP Molecular Weight on Membrane Morphology and Antibacterial Activity. *Desalination* **2011**, *273*, 72-80.

(38) Cui, L.; Chen, P.; Chen, S.; Yuan, Z.; Yu, C.; Ren, B.; Zhang, K. In Situ Study of the Antibacterial Activity and Mechanism of Action of Silver Nanoparticles by Surface-enhanced Raman Spectroscopy. *Anal. Chem.* **2013**, *85*, 5436-5443.

(39) Feng, Q.; Wu, J.; Chen, G.; Cui, F.; Kim, T.; Kim, J. A Mechanistic Study of the Antibacterial Effect of Silver Ions on Escherichia Coli and Staphylococcus Aureus. *J. Biomed. Mater. Res.* **2000**, *52*, 662-668.

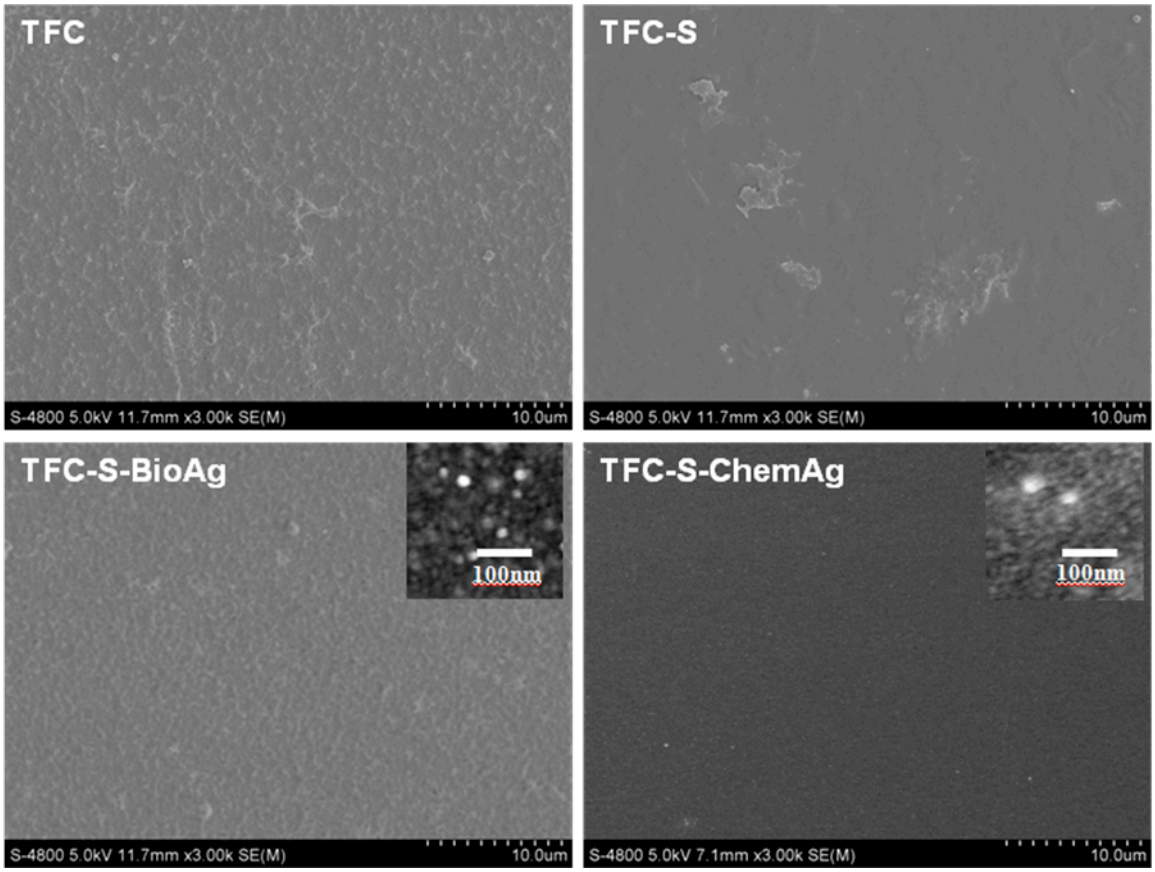

Fig.1. SEM images showing the surface morphologies of the pristin TFC, TFC-S, TFC-S-BioAg, and TFC-S-ChemAg membrane.

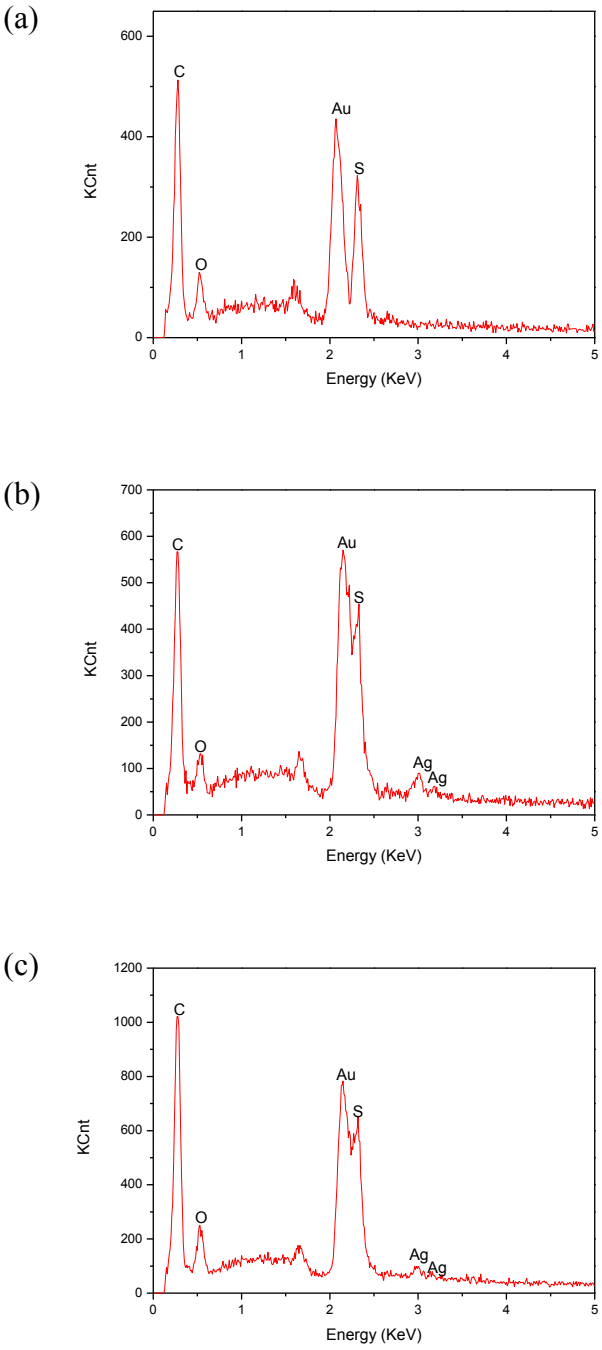

Fig.2. the energy dispersive X-ray spectra (EDX) of (a) the pristin TFC, (b) TFC-S-BioAg, and (c) TFC-S-ChemAg membrane.

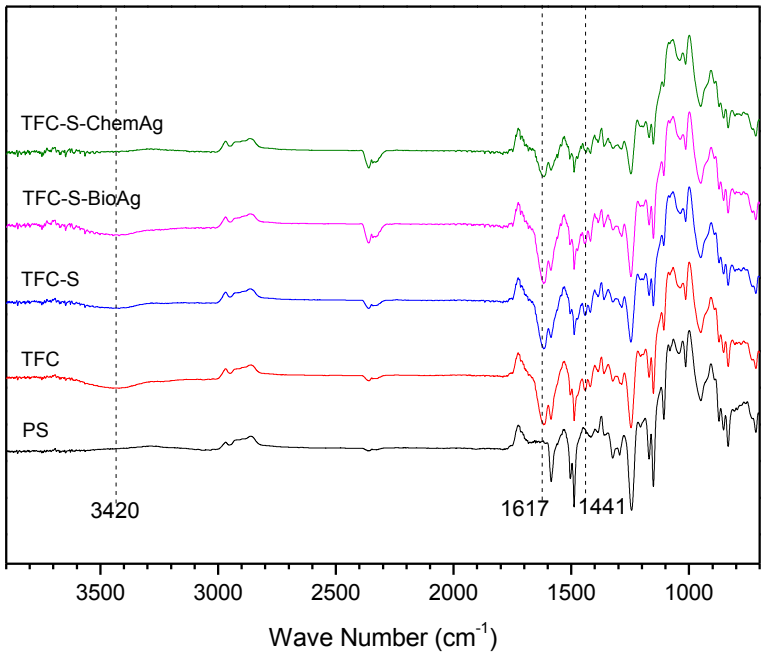

Fig.3. Comparison of FT-IR spectra of the pristin TFC, TFC-S, TFC-S-BioAg, and TFC-S-ChemAg membrane

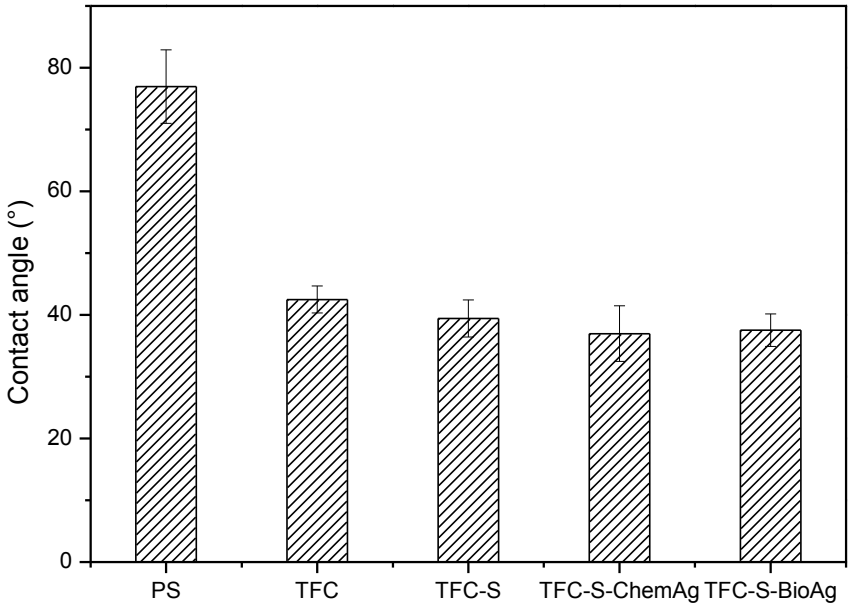

Fig.4. Water contact angles of the pristin TFC, TFC-S, TFC-S-BioAg, and TFC-S-ChemAg membrane surfaces

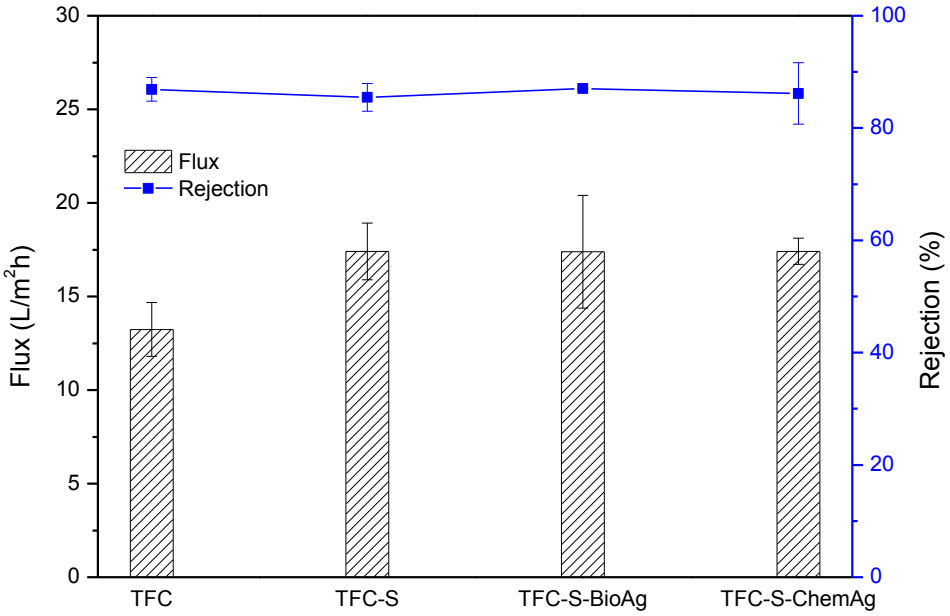

Fig.5. Water flux and salt rejection of the pristin TFC, TFC-S, TFC-S-BioAg, and TFC-S-ChemAg membrane samples.

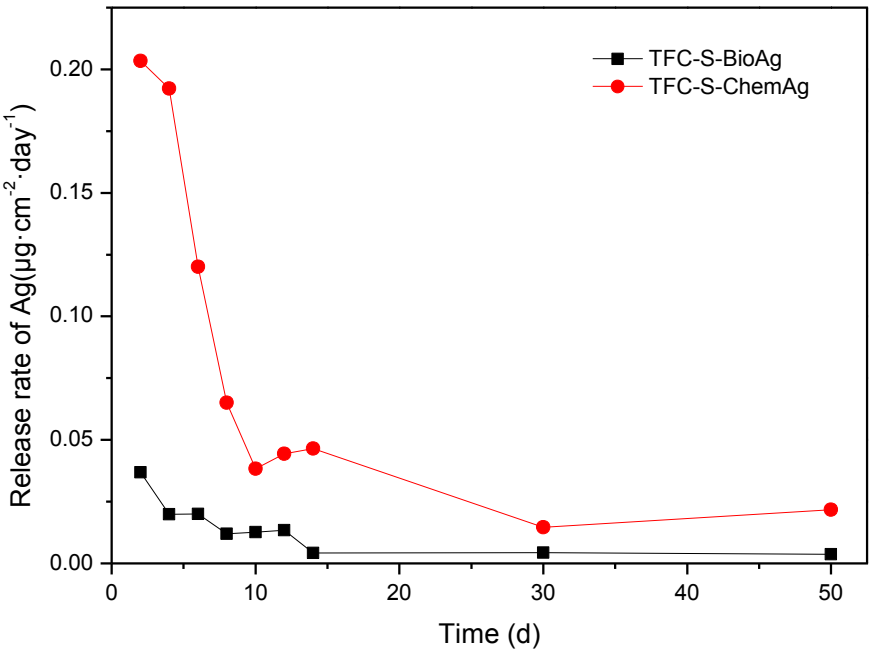

Fig.6. Silver release from the the TFC-S-Bio-Ag membrane and TFC-S-Chem-Ag membrane during 50 days soaking

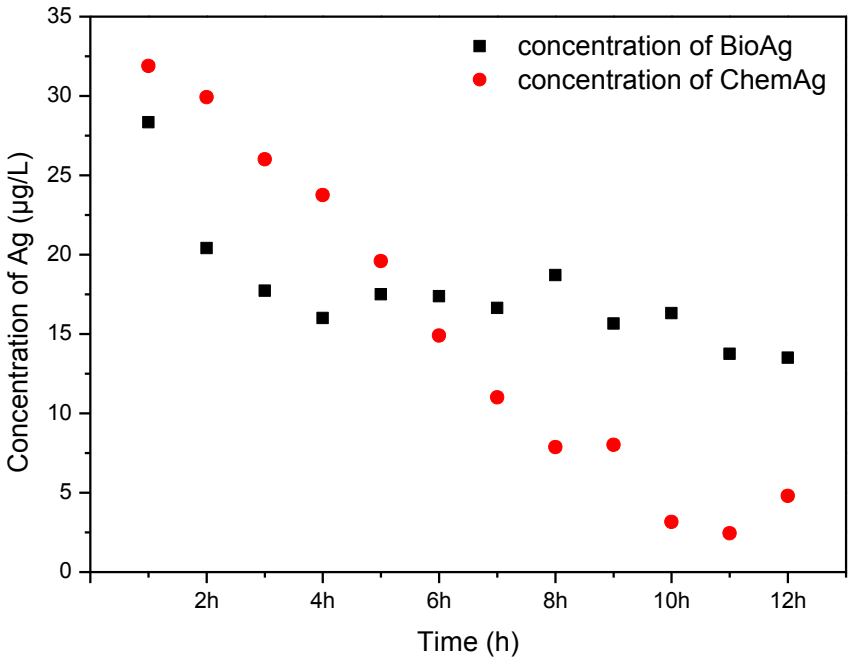

Fig.7. Silver release from the TFC-S-Bio-Ag membrane and TFC-S-Chem-Ag membrane during 12 h flow-through experiment

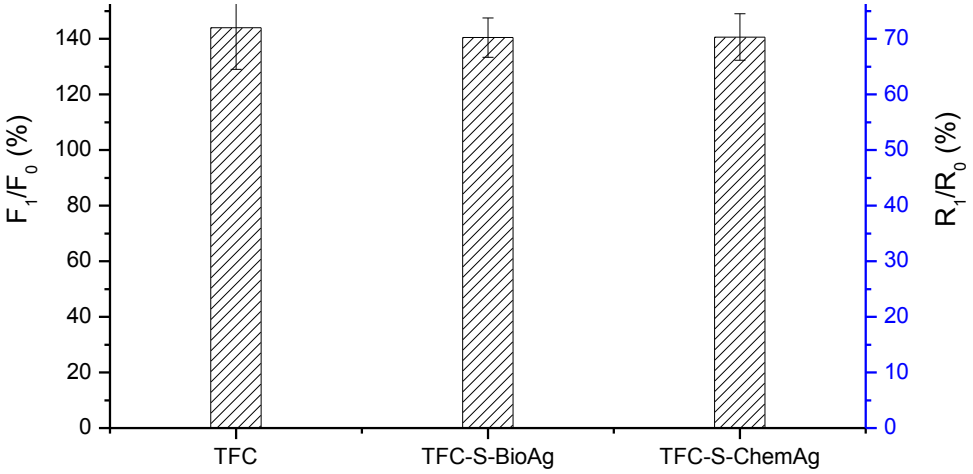

Fig.8. The effect of silver depletion (immersed in pure water for 4 months) on the change of pure water flux and salt rejection.

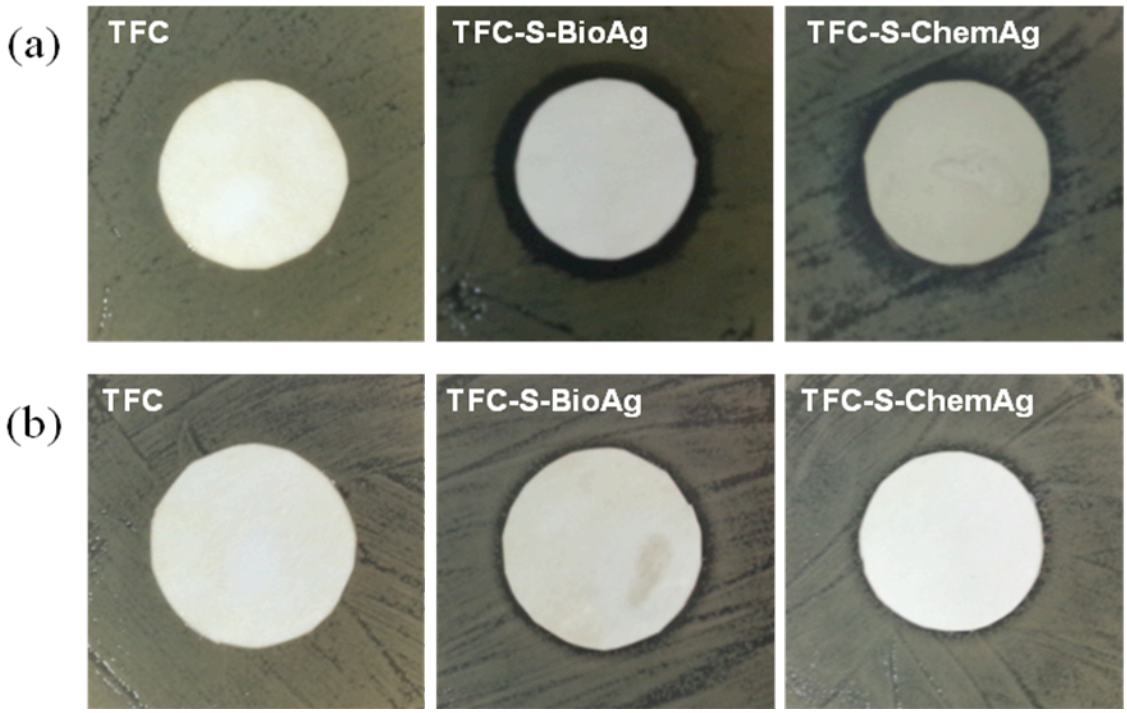

Fig.9. Anti-bacterial effect on (a) *P.aeruginosa* and (b) *E.coli* PA on the pristine TFC, TFC-S-BioAg, TFC-S-ChemAg membrane

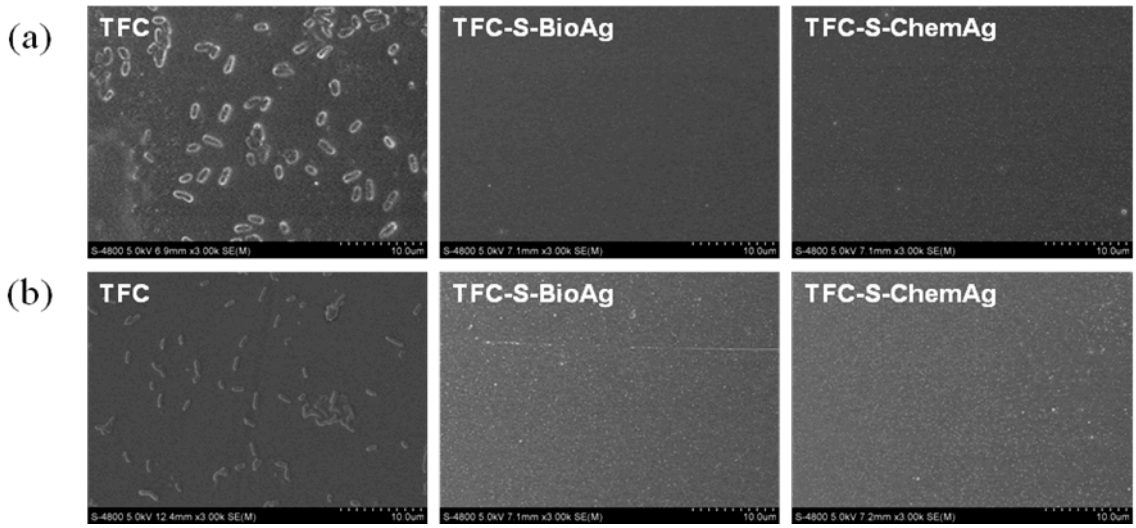

Fig.10. SEM images after batch incubation of the pristine TFC, TFC-S-BioAg, TFC-S-ChemAg membrane with (a) *P.aeruginosa* and (b) *E.coli*